Influence of Hall current and Joule heating on Electromagnetohydrodynamic flow transport through the heterogeneous circular microchannel

Amalendu Rana[1], V. Krishna Narla[2], Motahar Reza[3]

Department of Mathematics, School of Science,
GITAM Deemed to be University, Hyderabad 502329, India.
[1]amalmath94@gmail.com, [2]vnarla@gitam.edu, [3]mreza@gitam.edu.

ABSTRACT. The fabrication industry for micro-device technology in the chemical industry and biomedical instrumentation have grown up day by day. The fabrication process is becoming a tremendously challenging job for keeping the low price of devices and efficient performance. However, entire surfaces are typically heterogeneous, and microchannels with heterogeneous surfaces are commonly observed due to fabrication defects, material impurities, and chemical adsorption from solution. Such surface heterogeneity causes a non-uniform surface potential along the microchannel. In this paper, a theoretical investigation on the heat transfer characteristic of electrokinetic flow through a heterogeneous circular microchannel in magnetic field presence has been examined. The influence of the Hall Effect has been considered in this problem. Behavior in a circular microchannel with non-uniform surface potentials has been considered and analyzed. The analytical solution for the potential and numerical solution for the velocity distribution and temperature distribution has been obtained. The Hall Effect due to the heterogeneous surface on the non-uniform potential, velocity has been examined. Further, the joule heating parameter effect on heat transfer is discussed.

Keywords: Heterogeneous Surface, Hall Effect, EMHD, Microchannel, joule heating.

1 Introduction

The electrokinetic effects in the electric double layer (EDL) at the solid-liquid interface have been employed to develop various chemical and biomedical instruments [1-4]. The researchers study these phenomena' alleviating properties to manufacture a cheaper way with more precise microdevices like efficient micromixers, micro heat exchangers, and micropumps [5]. These components are needed to fabricate for recent technology microelectromechanical systems (MEMS), lab-on-a-chip devices, and high-performance cooling systems with a liquid as the working fluid, due to the inefficiency of the conventional air strategy [6] and large heat generation of microelectronic devices [7].

The fabricating of these devices is one of the great challenging tasks. The uniformity of surface during the electrokinetic fluid transport in the microchannels has been assumed in most problems [8 -9]. Nevertheless, it is interesting to note that the surface heterogeneity can quickly originate from fabrication defects or chemical adsorption onto microchannels. The relationship between protein adsorption and streaming potentials has been investigated by Norde et al. [10]. Analytical solution for electroosmotic flow through inhomogeneous charged surfaces is studied by Ajdari [11-12]. Ren and Li [13] numerically examined electroosmotic flow in heterogeneous circular microchannels with the surface potential's axial variation.

This present work investigates the effect of the magnetic field on the hydrodynamic characteristics of electroosmotic flow in a heterogeneous circular microchannel. In this study, a hydrodynamically fully developed mixed electroosmotic and pressure-driven flow in a circular microchannel being fabricated utilizing two different materials circumferentially has been considered in the presence of a magnetic field. Two different values of the zeta potential are assumed to model this problem. It is interesting to note that the governing non-dimensional equations for momentum and energy have been solved using numerical techniques. The velocity distribution, temperature distribution, and average velocity have been examined with various applied magnetic fields and other physical parameters. A comparison study has been illustrated to magmatic field effect and surface heterogeneous properties.

2 Problem Description and Mathematical Modelling

The electron magnetohydrodynamic (EMHD) flow performance of a pressure-driven flow in a heterogeneous circular microchannel with radius R is considered, which is to be circumferentially a composition of two different materials so that there are two different zeta potential values as shown in the figure-1, the one part of the wall composed of a material which is covered an angular degree of 2α and the rest part of the wall composed of another material which is covered the remaining $(2\pi - 2\alpha)$. For the sake of generality, in this investigation, α is considered as a variable and assumed that the flow is hydrodynamically fully developed flow of a Newtonian fluid. The electrolyte solution generates an EDL near the boundary wall, and the induced electric field in the opposite axial direction creates an electroosmotic flow. In the radial direction, the electromagnetic field is induced by the applied magnetic field and electric field. The polar, cylindrical coordinate (r, θ, z) is considered to describe this flow problem's governing equations. The total system is subjected to an applied magnetic field B_0 perpendicular to the fluid flow direction, and E_0 is imposed as an external transverse electric field from outside to inside.

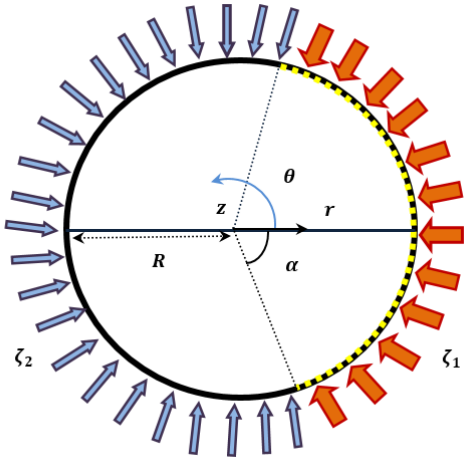

Fig-1: Physical sketch of the microchannel cross-section.

2.1. Potential distribution

The electroosmotic body force is proportional to the net electric charge within the liquid, which itself is a function of the ionic distribution. The first step of the present modeling is to obtain the electric potential distribution governed by the Poisson equation. Substituting for the net charge density in the Poisson equation using the Boltzmann distribution, assuming a solution with types of ionic species, the equation governing the electric potential distribution becomes

$$\nabla^2\psi = -\frac{\rho_e}{\varepsilon} \tag{1}$$

where ψ denotes the electric potential, ε represents the liquid permittivity, and ρ_e denotes net charge density, which is expressed by the given equation

$$\rho_e = -2n_0 ezsin\square(\frac{ez\psi}{k_B T_a}) \tag{2}$$

where n_0 represents the ion density, z is the valance, k_B denotes the Boltzmann constant. Here T represents the absolute temperature, and ε is the permittivity of the fluid.

Since ψ is too much small, so$(ez\psi/(k_B T)) << 1$, the term $sinh(ez\psi/(k_B\, T))$ can be estimated by $(ez\psi/(k_B\, T))$. This principle is cognized as Dybye-H$\ddot{u}$ckle linearization. After executing this Dybye-H$\ddot{u}$ckle linearization, finally, we rewrite that linearized Poisson equation using equ. (2):

$$\frac{1}{r}\frac{\partial}{\partial r}\left(r\frac{\partial\psi}{\partial r}\right) + \frac{1}{r^2}\frac{\partial^2\psi}{\partial\theta^2} = \kappa^2\psi \tag{3}$$

Where $\kappa = ez\left(\frac{2n_0}{\varepsilon k_B T}\right)^{\frac{1}{2}}$ is Dybye-H$\ddot{u}$ckle parameter and $1/\kappa$be the thickness of the EDL. The simplified form of the non-dimensionless electric potential equation and the pertinent boundary conditions can be written as

$$\frac{1}{r^*}\frac{\partial}{\partial r^*}\left(r^*\frac{\partial\psi^*}{\partial r^*}\right) + \frac{1}{r^{*2}}\frac{\partial^2\psi^*}{\partial\theta^2} = \omega^2\psi^* \tag{4}$$

$$\psi^* \neq \infty \; at \; r^* = 0\,, \psi^* = 1 - (1-\zeta_r)H(\theta-\alpha) \; at \; r^* = 1,$$

$$\frac{\partial\psi^*}{\partial\theta} = 0 \; at \; \theta = 0, \frac{\partial\psi^*}{\partial\theta} = 0 \; at \; \theta = \pi \tag{5}$$

where $\psi^* = \frac{\psi}{\zeta_1}, r^* = \frac{r}{R}$, and $\omega = \kappa R$. Here $\zeta_r = \zeta_2/\zeta_1$, is the ratio of the zeta potentials of the two-channel parts, ω is called the dimensionless electrokinetic width, and H is the Heaviside step function.

Using the separation of the variable method, the solution of potential distribution becomes

$$\psi^* = B_0 I_0(\omega r^*) + \sum_{n=1}^{\infty}\{B_n I_n(\omega r^*)\cos(n\theta)\} \tag{6}$$

where $B_0 = \frac{\alpha+(\pi-\alpha)\zeta_r}{\pi I_0(\omega)}$, $B_n = \frac{2(1-\zeta_r)\sin(n\theta)}{\pi n I_n(\omega)}$ and I_0 and I_n are the modified Bessel functions of the first kind with order zero and order n respectively.

2.2. Velocity Distribution:

The momentum equation for the Electromagnetohydrodynamic flow in a heterogeneous circular microchannel is written as a modified form of the Navier Stokes equation, which includes the combined electromagnetohydrodynamic body force ($\rho_e\vec{E}+\vec{J}\times\vec{B}$) where $\vec{E}$ is called electric field and $\vec{B}$ is the applied magnetic field. The current density ($\vec{J}$) and the Lorentz force both are affected by the Hall current. By considering hall current, the current density ($\vec{J}$) may be written as

$$\vec{J}+\frac{\sigma_e}{en_e}\left(\vec{J}\times\vec{B}\right)=\sigma_e(\vec{E}+\vec{U}\times\vec{B}), \tag{7}$$

where e be the fundamental charge of an electron, n_e is the number density of free electrons. Hence, for fully developed flow, the simplified form of the momentum conservation equation along the z-direction is derived as:

$$\mu\left(\frac{d^2u}{dr^2}+\frac{1}{r}\frac{du}{dr}\right)+\frac{\mu}{r^2}\frac{d^2u}{d\theta^2}-\frac{\mu u}{K}-\frac{dp}{dz}+\rho_eE_z+\frac{\sigma_eE_0B_0m}{1+m^2}-\frac{\sigma_eB_0^2u}{1+m^2}=0 \tag{8}$$

where u denotes the axial velocity, p is the pressure, K is called the permeability of the porous medium. $m=\sigma_e\,B_0/(e\,n_e)$ denotes the Hall parameter. The boundary conditions can written as

$$u\neq\infty\ at\ r=0\ ,u=0\ at\ r=R,$$

$$\frac{\partial u}{\partial\theta}=0\ at\ \theta=0,\frac{\partial u}{\partial\theta}=0\ at\ \theta=\pi \tag{9}$$

Substituting the value of ρ_e in equation (8) from equation (2) and introducing the dimensionless variables which are as follows:

$$u^*=\frac{u}{u_{HS}}\ ,r^*=\frac{r}{R},P=\frac{\left(-\frac{dp}{dz}\right)R^2}{\mu u_{HS}}\ ,\ Da=\frac{K}{R^2},Ha=B_0R\sqrt{\frac{\sigma_e}{\mu}}\ ,u_{HS}=-\frac{\varepsilon\zeta_1E_z}{\mu}\ \ ,S=\frac{E_0H}{u_{HS}}\sqrt{\frac{\sigma_e}{\mu}}$$

Hence, the dimensionless velocity distribution is derived as

$$\left(\frac{d^2u^*}{dr^{*2}}+\frac{1}{r^*}\frac{du^*}{dr^*}\right)+\frac{1}{r^{*2}}\frac{d^2u^*}{d\theta^2}-\left(\frac{Ha^2}{1+m^2}+\frac{1}{Da}\right)u^*+\omega^2\psi^*+\frac{HaSm}{1+m^2}+P=0 \tag{10}$$

where u_{HS} is the Helmoholtz-Smoluchowski velocity with characteristic electric field strength E_z, Da represents Darcy number, Ha represents Hartmann number which is indicating the strength of the applied magnetic field B_0, S represents the strength of the transverse electric field E_0. After non-dimensionalization, the boundary conditions reduce to as follows:

$$u^*\neq\infty\ at\ r^*=0\ ,u^*=0\ at\ r^*=1,$$

$$\frac{\partial u^*}{\partial\theta}=0\ at\ \theta=0,\frac{\partial u^*}{\partial\theta}=0\ at\ \theta=\pi \tag{11}$$

By solving the equation (10) subject to the boundary condition (11), we can find the dimensionless velocity distribution. Further, the dimensionless average velocity can be obtained as

$$u_{av}^{*} = \frac{\int_0^{\pi}\int_0^{1} u^{*} r^{*} dr^{*} d\theta}{\int_0^{\pi}\int_0^{1} r^{*} dr^{*} d\theta} \tag{12}$$

2.3. Temperature Distribution:

The governing equations of energy equation for thermally fully developed flow is expressed as

$$\rho C_P u \frac{\partial T}{\partial z} = k\left\{\frac{1}{r}\frac{\partial}{\partial r}\left(r\frac{\partial T}{\partial r}\right) + \frac{\partial^2 T}{\partial \theta^2}\right\} + \sigma_e E_z^2 + \frac{\sigma_e B_0^2 u^2}{1+m^2} \tag{13}$$

where, T is the local temperature of the liquid, and k is the thermal conductivity of the fluid and (ρC_P) is called the heat capacity per unit volume of the fluid. Here the last two terms indicate the volumetric heat generation due to the applied body force. The boundary condition associated with equation (13) read

$$T \neq \infty \; at \; r = 0 \, , \, k\frac{\partial T}{\partial r} = q_1 - (q_1 - q_2)H(\theta - \alpha) \; at \; r = R$$

$$\frac{\partial T}{\partial \theta} = 0 \; at \; \theta = 0, \frac{\partial T}{\partial \theta} = 0 \; at \; \theta = \pi \tag{14}$$

where q_1 and q_2 are the inward wall heat flux of part 1 and 2, respectively. Introducing the non-dimensional temperature $T^{*} = \frac{k(T-T_w)}{q_w R}$ where T_w is the channel wall temperature and q_w is the constant wall heat flux. Further, for thermally fully developed flow under imposed constant wall heat flux, one may write $\frac{\partial T}{\partial z} = \frac{dT_w}{dz} = \frac{dT_b}{dz} = constant$ and $\frac{d^2T}{dz^2} = 0$ in which T_b is the bulk mean temperature. The overall energy balance of an elementary control volume of the fluid with the length of duct dx gives the following expression:

$$\frac{dT_b}{dz} = \frac{1}{(\rho C_P) R u_m}\left[2\{\alpha q_1 + (\pi - \alpha)q_2\} + \frac{\sigma_e}{1+m^2}\left\{E_z^2 R + \int_0^R B_0^2 u^2 r dr\right\}\right] \tag{15}$$

Then the bulk mean temperature gradient can be obtained as

$$\frac{dT_b}{dz} = \frac{\gamma_1}{\rho C_P} = constant. \tag{16}$$

Where $\gamma_1 = \frac{1}{R u_m}\left\{2\{\alpha q_1 + (\pi - \alpha)q_2\} + \frac{\sigma_e}{1+m^2}\{E_S^2 R + \frac{B_0^2 \beta_1}{R}\right\}$, $\beta_1 = \int_0^R u^2 \, r dr$ and $u_m = \frac{\int_0^{2\pi}\int_0^R u r dr d\theta}{\pi R^2}$ which is called axial mainstream velocity. The following dimensionless parameters are introduced to make dimensionless the equation (13)

$\gamma = \left(\frac{\gamma_1 u_{HS} R}{q_1}\right), Br = \frac{\mu u_{HS}}{h q_1}$, $s_J = \frac{\sigma_e E_S^2 R}{q_1}$.

Where γ is the ratio of the heat generated by the interaction of the electric and magnetic fields to heat conduction, Br is the Brinkman number, which describes the ratio of heat produced by viscous dissipation and heat transport by molecular conduction, S_J is the joule heating due to heat conduction. Then by using (15), the non-dimensional form of the equation (13) is obtained as

$$\left(\frac{d^2T^{*}}{dr^{*2}} + \frac{1}{r^{*}}\frac{dT^{*}}{dr^{*}}\right) + \frac{1}{r^{*2}}\frac{d^2T^{*}}{d\theta^2} = \gamma Pe u^{*} - \frac{Br Ha^2 u^{*2}}{1+m^2} - \frac{S_j}{1+m^2} \tag{17}$$

The corresponding non-dimensional boundary conditions are expressed as

$$T^{*} \neq \infty \; at \; r^{*} = 0 \, , \, \frac{\partial T^{*}}{\partial r} = 1 - (1 - q_r)H(\theta - \alpha) \; at \; r^{*} = 1$$

$$\frac{\partial T^*}{\partial \theta} = 0 \; at \; \theta = 0, \frac{\partial T^*}{\partial \theta} = 0 \; at \; \theta = \pi \tag{18}$$

where $q_r = q_2/q_1$ is the heat flux ratio. Further, equation (17) is solved numerically and obtained the dimensionless temperature distribution.

3 Results and Discussions

The differential equation (10) and (17) subject to the boundary conditions (12) and (18) respectively has been evaluated numerically which is conducted in Mathematica-12 NDSolve algorithm and the average velocity is evaluated by using numerical integration method. The results are visualized graphically for the influence of the pertinent parameters in fig-2-6. Figure 2 display the potential distribution for various values ζ_r (the ratio of the zeta potentials of the two channel parts). Most interesting that the dimensionless potential distribution is very much affected by the zeta potential ratio and it is visible near to the channel wall.

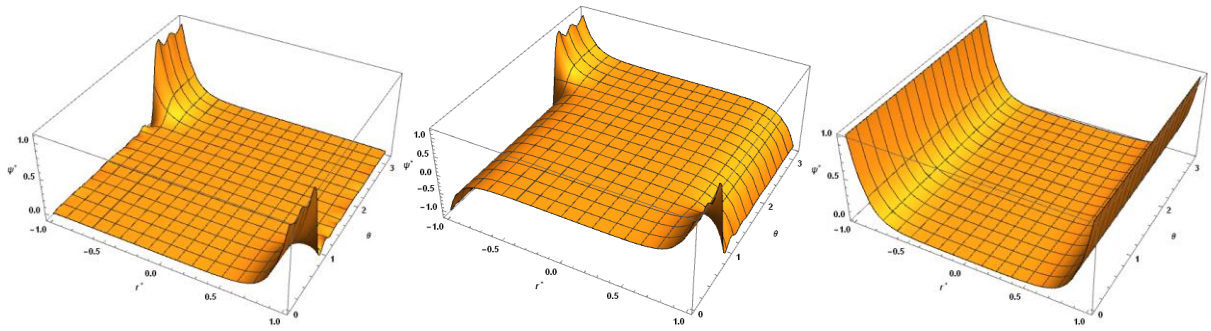

(a) $\zeta_r = -1$ (b) $\zeta_r = 0$ (c) $\zeta_r = 1$

Fig-2: Potential distribution plots for different ζ_r with $\omega = 5, \alpha = \pi/4$.

The dimensionless average velocity plots for the variation of different parameters are given in figure 3-6. The dimensionless average velocity with dimensionless Debye-Huckel parameter (ω) at different values of other parameters are illustrates in fig-3. The average velocity generally increases with the increment of ω and the zeta potential ratio, which is displayed in fig-3(a). The increasing trend occurs because of the concentration of the body force near to the channel wall due to electroosmotic effect. Figure-3(b) depicted that the average velocity decreases with increases of Hartmann number. The magnitude of the Hartmann number indicates the strength of the applied magnetic field, which is acting as a Lorentz force on the fluid particles. The fluid velocity reduces because of the Lorentz force, which is acting as retarding force on the flow. It also can be found from Figure 3(c) that the average velocity is decreasing with increasing Darcy number Da when other physical parameters are constant. The porosity of the circular microchannel reduces the velocity of fluid flow. So when Darcy number increases, the permeability of the porous medium increases, which causes a decrease of the average velocity of a fluid. The impact of the Hall parameter on the average velocity with ω can be found in figure 3(d). This figure shows that as the Hall parameter increases, the average velocity of the fluid is reduced. The physics behind this observation is that the electrical conductivity of the fluid reduces as the Hall parameter increases and thereby, the applied magnetic field effect reduces the fluid velocity.

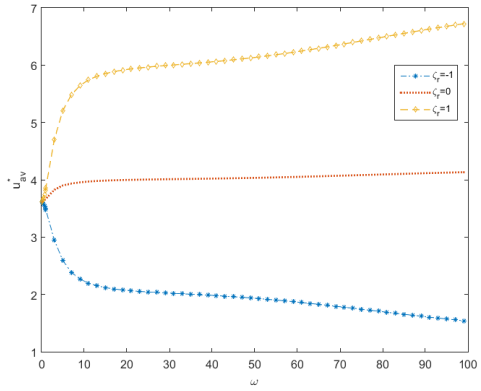

(a)

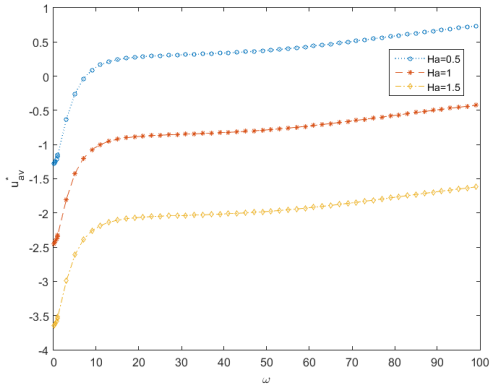

(b)

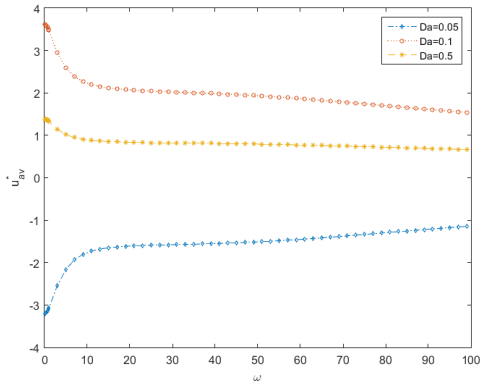

(c)

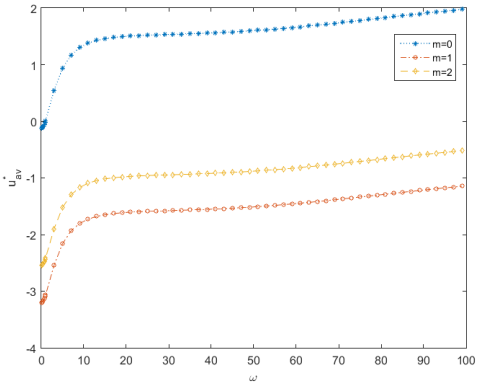

(d)

Fig-3: Avg. Velocity vs ω plots for different values of Ha, (b) for different values of Da and (c) for different values of Hall parameter, (d) for different values ζ_r, while keeping $\alpha = \frac{\pi}{4}, S = 50, \zeta_r = -1$.

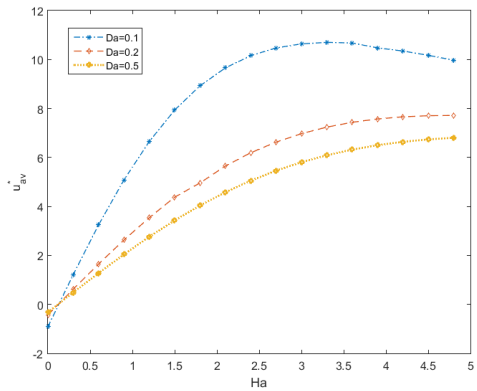

(a)

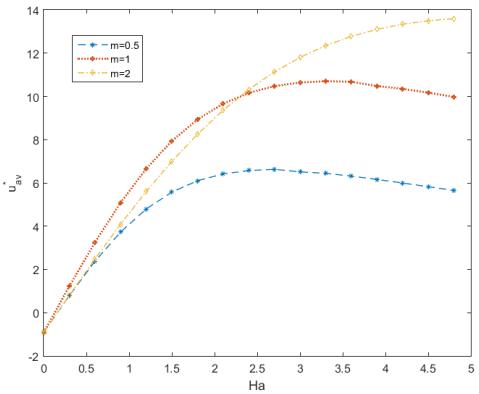

(b)

Fig-4: Avg. Velocity vs Ha plots (a) for different values of Da and (b) for different values of Hall parameter, while keeping $\omega = 5, \alpha = \frac{\pi}{4}, S = 50, \zeta_r = -1$.

Figure 4 depicts the average velocity plots with Hartmann's number for different values of Darcy number and Hall parameter. The average velocity is decreasing with the increment of Darcy number, which is represented in figure 4(a). The permeability of the porous medium

increases the value of Darcy number; as a result, the porosity reduces the flow velocity. It can be observed from figure 4(b) that the increment of the Hall parameter enhanced the average velocity. The increment of Hall parameter reduces the electric conductivity of the fluid and therefore the applied magnetic damping effect reduces and as a result fluid velocity is enhanced. The average velocity increases with the enhancement of the transverse electric field that is displayed in figure 5. The strength of the transverse electric field is acting as a flow aiding force. As a result the average velocity of the flow is improved with the increment of S. The increase of Hartmann number enhanced the average velocity rapidly with the increment of the transverse electric field, which is shown in figure 5(a). A similar physical phenomenon is observed for the decrement of Darcy number, which is represented in figure 5(b), but it is interesting to know that for the low value of S the average velocity is enhanced with the increases of Darcy number. The average velocity is increasing with the increases of pressure gradient, which is shown in figure 6. The average velocity increases with the increment of Hartmann number and hall parameter, which are displayed in figure 6(a) and 6(c), respectively but there is a reduction in average velocity with the increment of Darcy number, which is depicted in figure 6(b).

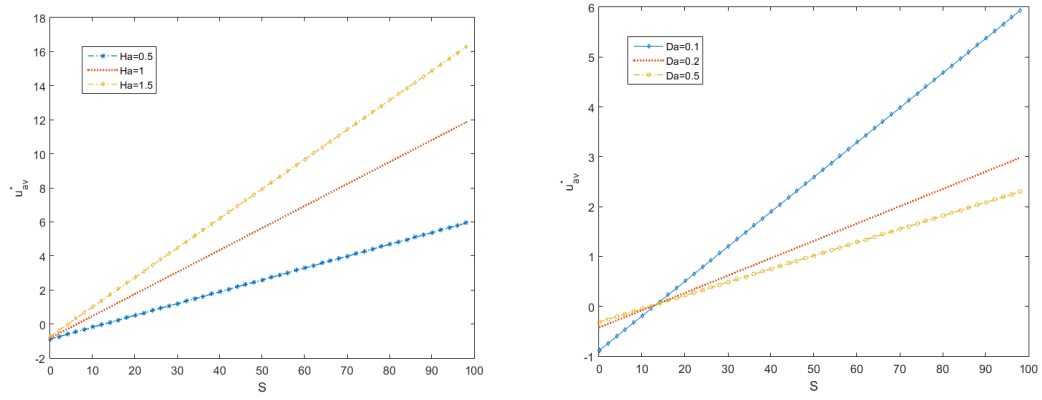

(a) (b)

Fig-5: Avg. velocity vs S plots (a) for different values of Ha and (b) for different values Da, while keeping $\omega = 5, \alpha = \frac{\pi}{4}, m = 1, \zeta_r = -1$.

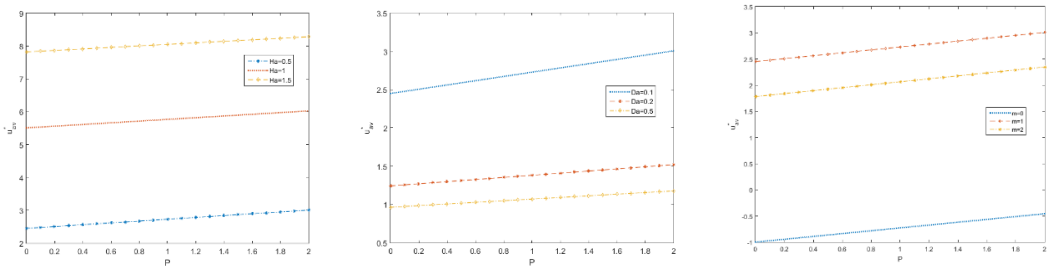

(a) (b) (c)

Fig-6: Avg. Velocity vs P plots (a) for different values of Ha, (b) for different values of Da and (c) for different values of Hall parameter, while keeping $\omega = 5, \alpha = \frac{\pi}{4}, S = 50, \zeta_r = -1$.

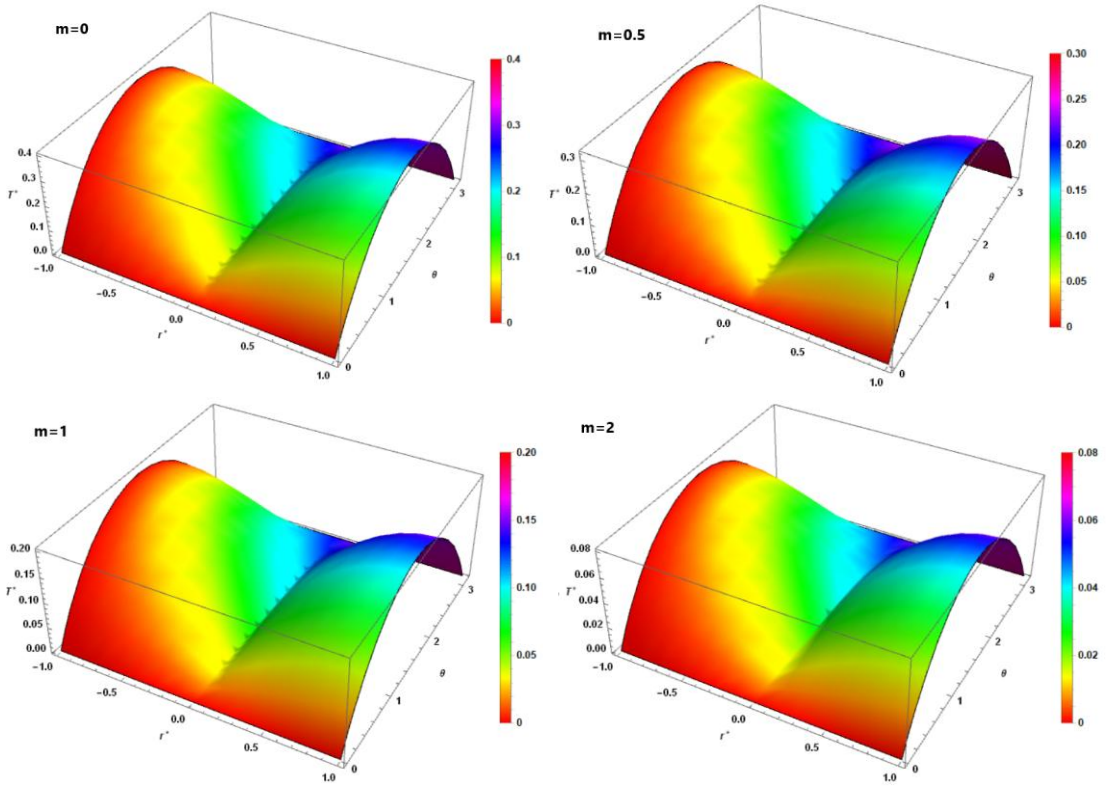

Fig-7: Temperature plots for different values of Hall parameter, while keeping $\omega = 5, \alpha = \frac{\pi}{4}, S = 50, \zeta_r = -1, S_j = 1, Pe = 1, Br = 0$.

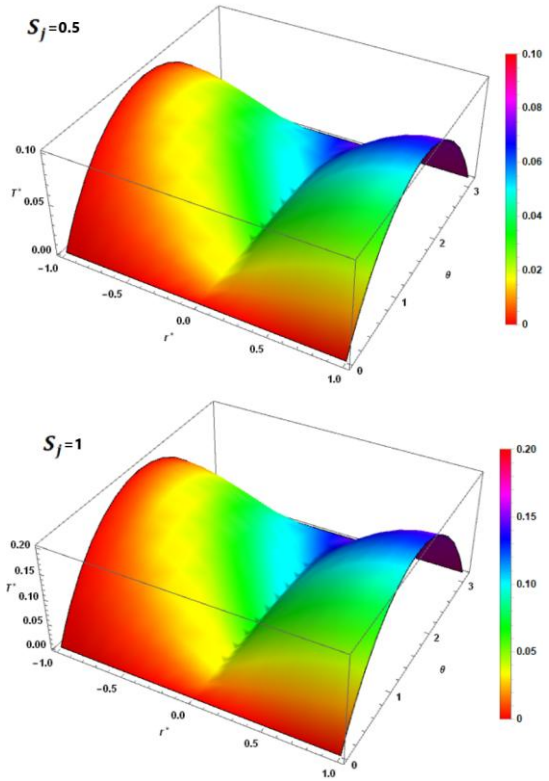

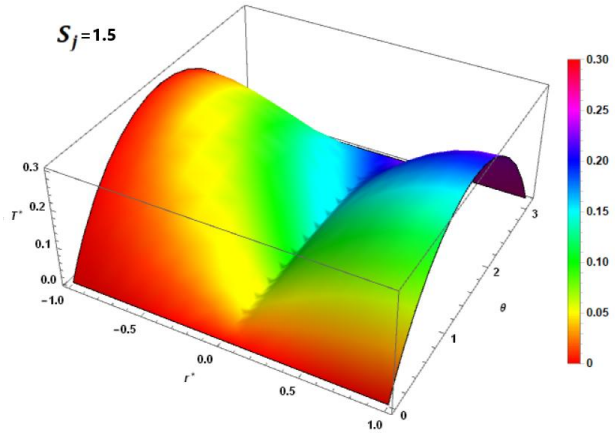

Fig-8: Temperature plots for different values of joule heating parameter, while keeping $\omega = 5, \alpha = \frac{\pi}{4}, S = 50, \zeta_r = -1, m = 1, Pe = 1, Br = 0.$

The effect Hall current and joule heating on temperature distribution is delineated in figure 7 and figure 8. It is demonstrated in figure 7 that the temperature profile decreased with the increasing trend of Hall current effect. It also observed that the temperature is maximum for $m = 0$ i.e. non-existing case of Hall current. In addition, when the joule heating parameter is increasing, then the temperature is increasing which is displayed in the figure 8.

4 Conclusions :

From this investigation, the potential distribution and velocity distribution is analyzed for the EMHD flow through a circular microchannel with porous medium under the influence of Hall current. The following observations can be drawn from this numerical study:

- The average velocity is inversely proportional to the applied magnetic field, and it is increasing rapidly for small values of Hartmann number.
- Due to the impact of Hall current, there is a rise in the average velocity profile.
- Flow-through the porous microchannel reduces with an increase of Darcy number.

Acknowledgments

This work was supported by SERB, Govt of India. (Grant File No. EMR/2016/006383). The authors would like to acknowledge this support.

5 References

[1] Harrison, J. D.; Fluri, K.; Seiler, K.; Fan, Z. H.; Effenhauser, C. S.; Manz, A. *Science* **1993**, *261*, 895.

[2] Blackshear, P. J. *Sci. Am.* **1979**, *241*, 52

[3] Penn, R. D.; Paice, J. A.; Gottschalk, W.; Ivankovich, A. D. *J. Neurosurg.* **1984**, *61*, 302.

[4] Rice, C. L.; Whitehead, R. *J. Phys. Chem.* **1965**, *69*, 4017.G

[5] Karniadakis, A. Beskok, N. Aluru, Springer Science & Business Media, 2005.

[6] L. Sauciuc, G. Chrysler, R. Mahajan, M. Szleper, in: Semiconductor Thermal Measurement and Management Symposium, 2003. Ninteenth Annual IEEE, IEEE, 2003, pp. 74-81.
[7] D. Ansari, K.-Y. Kim, International Journal of Thermal Sciences, 134 (2018) 27-39.
[8] Yang, J.; Kwok, D. Y. *J. Chem. Phys.* **2003**, *118*, 354.
[9] Yang, J.; Kwok, D. Y. *Langmuir* **2003**, *19*, 1047
[10] Norde, W.; Rouwendal, E. E. *J. Colloid Interface Sci*. **1990**, *139*,169.
[11] Ajdari, A. *Phys. Rev. Lett.* **1995**, *75* (4), 755.
[12] Ajdari, A. *Phys. Rev. E* **1996**, *53* (4), 4996.
[13] Ren, L.; Li, D. *J. Colloid Interface Sci.* **2001**, *243*, 255.